A research of patient-specific flow boundary condition in noninvasive coronary fractional flow reserve

*** Q.Q. Yang[1], † A.K. Qiao[1], Y. Hou[2], and Y. Ma[2]**

[1]College of Life Science and Bioengineering, Beijing University of Technology, Beijing 100124, China
[2]Shengjing Hospital of China Medical University, Shenyang 110001, China

* Presenting author: yangqq1990@foxmail.com
† Corresponding author: qak@bjut.edu.cn

Abstract

Background: The clinical shortage problems of invasive fractional flow reserve (FFR) can be effectively solved by computed tomography angiography-derived fractional flow reserve (FFR_{CT}), which is a noninvasive functional parameter for the diagnosis of coronary artery disease. However, the accuracy of FFR_{CT} is one of the main problems. The boundary condition is the main factor affecting the accuracy of the FFR_{CT}, while few researches are about this issue.

Object: This study focuses on the settings of the individualized boundary condition for the calculation of FFR_{CT} in order to improve its accuracy.

Methods: A mathematical model of patient-specific flow boundary condition was presented. Firstly, a vessel volume-based method to calculate flow division fraction was presented for the left anterior descending (LAD) artery, the left circumflex (LCX) artery, and the right coronary artery (RCA) based on the "form-function" relationships. Then, the flow division fraction of each coronary outlet could be calculated by combining the shear stress formula of the Hagen-Poiseuille flow, the uniform shear hypothesis and Murray's law. Next, a mathematical model of coronary blood flow at hyperemia (Q_{cor}) was presented. Some independent physiological parameters of coronary blood flow were selected, including the myocardial mass (M_L), diastolic blood pressure (P_D) and heart rate (HR). The model was expressed as: $Q_{cor} = kHR[-0.568\ln(HR) + 3.246]P_D(\frac{M_L}{0.85})^{0.75}$. Finally, the flow rate of each coronary outlet can be calculated by integrating the model and the flow division fraction. Sixteen cases of patients with coronary stenosis were employed for finite element analyses.

Results: (1) The coronary flow divisions for LAD, LCX, and RCA were 32.9%, 20.6%, and 46.5% respectively, and they were almost identical to those from clinical measurement. (2) The mean values of the ratio of total coronary blood flow in cardiac output and myocardial blood flow of 16 patients were 16.97% and 4.07 mL/min/g respectively, which were in accordance with the rule of medical statistics. (3) The diagnostic accuracy of simulation FFR_{CT} was higher than CT alone (85% vs. 65%) with the reference of invasive FFR, and there was a good agreement between FFR_{CT} and FFR.

Conclusions: The coronary FFR_{CT} has good consistency with invasive FFR under the patient-specific flow boundary condition. This study offers a new way for improving FFR_{CT} accuracy, as well as promotes the clinical application of FFR_{CT}.

Keywords: Coronary artery stenosis, Fractional flow reserve, Hemodynamics, Patient-specific boundary condition

Introduction

The clinical shortage problems of invasive fractional flow reserve (FFR) [3] can be effectively solved by computed tomography angiography-derived fractional flow reserve (FFR_{CT}) [1-2], which is a noninvasive functional parameter for the diagnosis of coronary artery disease. FFR_{CT} has been widely concerned by clinicians and researchers in recent years. The diagnostic performance of FFR_{CT} has been investigated experimentally by some multicenter studies, including DISCOVER-FLOW (Diagnosis of Ischemia-Causing Stenoses Obtained Via Noninvasive Fractional Flow Reserve) [4-5]、DeFACTO (Determination of Fractional Flow Reserve by Anatomic Computed Tomographic Angiography) [6-9] and NXT (Analysis of Coronary Blood Flow Using CT Angiography: Next Steps) [10-12], comprising a total of 609 patients and 1050 vessels. The latest trail showed that the accuracy of FFR_{CT} was 81% [11], which is good enough for the result of simulation but not good enough for clinical applications.

The accuracy of FFR_{CT} is the most important problem limiting its clinical application. The main factor affecting the accuracy of the FFR_{CT} is the boundary condition, while few researches are about this issue.

The boundary condition is the driving condition for the coronary blood flow, and directly determines the state of blood flow. The calculation of total coronary blood flow is used for the simplified settings of the boundary condition [1]. In previous studies, the calculation of total coronary blood flow is based on the scaling relation between myocardial mass and coronary blood flow [13]. However, myocardial mass is not the only factor affecting coronary blood flow. There are individual differences in the correlation between myocardial mass and total coronary blood flow. Heart rate and aortic peak pressure were considered as input in the mathematical model of coronary blood flow presented by Arthurs et al [14]. This model can provide patient-specific estimates of coronary blood flow changes between rest and exercise. Except for heart rate and aortic peak pressure, left-ventricular pressure-volume loop was also considered as input parameter which was not easy to detect. So, an accurate and non-invasive method for obtaining total coronary blood flow is a problem that must be faced to improve the accuracy of FFR_{CT} calculation.

In view of the above reasons, this study presents a mathematical model of noninvasive simulation of coronary blood flow, and explores the individualized settings of the boundary condition for FFR_{CT} calculation in order to improve its accuracy.

Methods

Study population

16 patients with steady coronary artery disease were included in our study. The following were reasons for exclusion from the study: (1) myocardial damage or recent myocardial infarction (within one month); (2) left ventricular dysfunction; (3) significant 3-vessel disease; (4) poor quality CT images. All patients underwent coronary computed tomographic angiography (CCTA) and coronary FFR.

Flow division to coronary major branches

Several morphological (diameter, length, and volume) and functional (flow) parameters of the coronary arterial tree in relation to myocardial mass were quantified in animal experiments in vitro by Choy et al [13]. The results showed that arterial volume is linearly related to regional myocardial mass, whereas the sum of coronary arterial branch lengths, vessel diameters, and volumetric flow show a 3/4, 3/8, and 3/4 power-law relationship, respectively. This is consistent with the earlier experimental results of Seiler et al [15-16]. Based on a physiological observation that longer coronary arteries have more daughter branches feeding a larger mass of cardiac muscle, Lee et al presented a vessel length-based method calculating the coronary flow division over coronary major arteries [17]. Given that the volume parameter contains the diameter and the length, we proposed a vessel volume-based method to calculate flow division over coronary major arteries.

Given that arterial volume is linearly related to regional myocardial mass, the regional myocardial mass of the left anterior descending (LAD) artery, the left circumflex (LCX) artery, and the right coronary artery (RCA) can be described accordingly as equation (1).

$$M_{LAD} = \alpha V_{vessel\ LAD};\ M_{LCX} = \alpha V_{vessel\ LCX};\ M_{RCA} = \alpha V_{vessel\ RCA} \tag{1}$$

where M_{LAD}, M_{LCX}, and M_{RCA} represents the regional myocardial mass of LAD, LCX, and RCA respectively; $V_{vessel\ LAD}$, $V_{vessel\ LCX}$, and $V_{vessel\ RCA}$ represents the vessel volume of LAD, LCX, and RCA respectively; α is a constant scale coefficient.

The volumetric flow showed a 0.75 power-law relationship with myocardial mass, so we can get the equation (2).

$$Q_{LAD} = \beta M_{LAD}^{0.75};\ Q_{LCX} = \beta M_{LCX}^{0.75};\ Q_{RCA} = \beta M_{RCA}^{0.75} \tag{2}$$

where Q_{LAD}, Q_{LCX}, and Q_{RCA} represents the volumetric flow of LAD, LCX, and RCA respectively; β is a constant scale coefficient.

Then, equation (3) can be deduced from the above two equations. Namely, the volumetric flow shows a 0.75 power-law relationship with vessel volume.

$$Q_{LAD} = \alpha\beta V_{vessel\ LAD}^{0.75};\ Q_{LCX} = \alpha\beta V_{vessel\ LCX}^{0.75};\ Q_{RCA} = \alpha\beta V_{vessel\ RCA}^{0.75} \tag{3}$$

So we can deduce the flow division ratio over coronary major arteries as equation (4).

$$Q_{LAD} : Q_{LCX} : Q_{RCA} = V_{vessel\ LAD}^{0.75} : V_{vessel\ LCX}^{0.75} : V_{vessel\ RCA}^{0.75} \tag{4}$$

Flow division to each coronary outlet

The total coronary blood flow is the sum of blood flow over LAD, LCX, and RCA as equation (5).

$$Q_{cor} = Q_{LAD} + Q_{LCX} + Q_{RCA} \tag{5}$$

So the flow division of LAD, LCX, and RCA is described as equation (6) respectively.

$$\left.\begin{aligned} Q_{LAD} &= \frac{V_{vessel\ LAD}^{0.75}}{V_{vessel\ LAD}^{0.75} + V_{vessel\ LCX}^{0.75} + V_{vessel\ RCA}^{0.75}} Q_{cor} \\ Q_{LCX} &= \frac{V_{vessel\ LCX}^{0.75}}{V_{vessel\ LAD}^{0.75} + V_{vessel\ LCX}^{0.75} + V_{vessel\ RCA}^{0.75}} Q_{cor} \\ Q_{RCA} &= \frac{V_{vessel\ RCA}^{0.75}}{V_{vessel\ LAD}^{0.75} + V_{vessel\ LCX}^{0.75} + V_{vessel\ RCA}^{0.75}} Q_{cor} \end{aligned}\right\} \tag{6}$$

Ideally, the blood flow in a vessel is proportional to the 3rd power of the vessel diameter according to Poiseuille's solution and Murray's law [18] as equation (7).

$$Q = \frac{\pi d^3}{4}\sqrt{\frac{\lambda}{\mu}} \tag{7}$$

where Q is the flow rate through a blood vessel, d is its diameter, μ is the fluid viscosity, λ is a constant, and it represents the energy consumed by the metabolism of unit volume.

We set *a*, *b*, and *c* as the diameter of each branch of LAD, LCX, and RCA respectively. The flow rate of each branch can be inferred from equation (7).

$$\left.\begin{aligned} Q_{LAD-\mathrm{j}} &= Q_{LAD}\frac{a_j^{\,3}}{\sum_{i=1}^{n} a_i^{\,3}} \\ Q_{LCX-\mathrm{j}} &= Q_{LCX}\frac{b_j^{\,3}}{\sum_{i=1}^{m} b_i^{\,3}} \\ Q_{RCA-\mathrm{j}} &= Q_{RCA}\frac{c_j^{\,3}}{\sum_{i=1}^{s} c_i^{\,3}} \end{aligned}\right\} \tag{8}$$

However, the coronary artery model reconstructed from CCTA was not completely matched with Murray's law, thus a revision has been made in equation (8). As shown in Figure 1, the flow division of each branch was calculated in the direction of blood flow according to the classification of vascular branches.

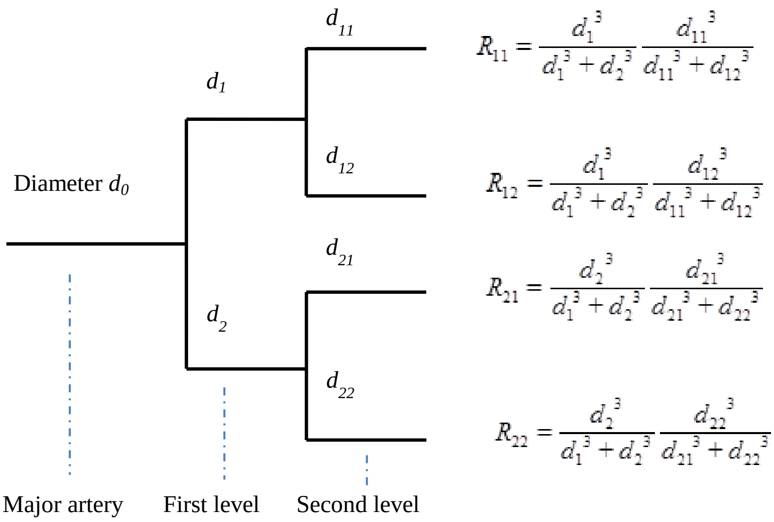

Figure 1. Schematic diagram of diversion ratio calculation (*R* presents diversion ratio)

Model of coronary blood flow

Coronary artery is the vascular system supplying blood for the myocardium. Some vessels buried deep within the myocardium will be pressed during cardiac systole, which will affect coronary blood flow. The blood flow will come to the climax at early diastole, and then decrease slowly [19]. In general, coronary blood flow during left ventricular systole is only 20~30% of those during diastole, and which will be smaller when myocardial contraction strengthens.

Some independent physiological parameters of coronary blood flow were selected based on the discussion above, including the myocardial mass, diastolic blood pressure and heart rate.

Myocardial mass. The scaling laws between coronary blood flow and the myocardial mass can be described as equation (9).

$$Q_{cor} \propto M^{0.75} \tag{9}$$

In a broad sense, the myocardium includes right ventricular myocardium, atrial myocardium and other myocardial tissue besides the left ventricular myocardium. The left ventricular myocardial mass accounts for about 85% of the total myocardial mass[20-21]. So the scaling law can be revised as equation (10).

$$Q_{cor} \propto \frac{M_L}{0.85}^{0.75} \tag{10}$$

Diastolic blood pressure. The coronary perfusion is mainly affected by the diastolic blood pressure since coronary blood flow perfusion is mainly in diastole. According to Poiseuille's law,

$$Q = \frac{\pi r^4}{8\eta L}\Delta P \tag{11}$$

and coronary anatomy, the perfusion pressure is as equation (12),

$$\Delta P = P_D - P_{Ra} \tag{12}$$

where P_D is the aortic diastolic blood pressure, and P_{Ra} is the right atrial pressure (-2~10 mmHg). For the sake of simplification, the perfusion pressure was set as the aortic diastolic blood pressure in this study. So the relationship between coronary blood flow and the diastolic blood pressure can be described as equation (13).

$$Q_{cor} \propto P_D \tag{13}$$

Heart rate. Effective perfusion time is another factor affecting coronary blood flow. The diastole of a cardiac cycle is the time of coronary blood flow perfusion[19]. Diastolic duration is relatively compressed with the increase of heart rate (Figure 2)[22]. According to the correlation between heart rate and diastolic duration, the perfusion time pre minute can be described as equation (14).

$$T = HR\left[-0.568\ln(HR) + 3.246\right] \tag{14}$$

So the relationship between coronary blood flow and the heart rate can be described as equation (15).

$$Q_{cor} \propto HR\left[-0.568\ln(HR) + 3.246\right] \tag{15}$$

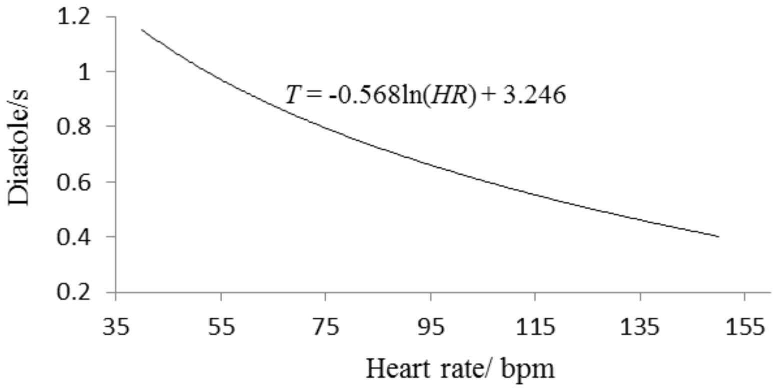

Figure 2. Correlation between left ventricular diastole and heart rate during a cardiac cycle

From the discussion above, the mathematical model of coronary blood flow during hyperemia with adenosine can be established as equation (16).

$$Q_{cor} = kHR\left[-0.568\ln(HR) + 3.246\right]P_D\left(\frac{M_L}{0.85}\right)^{0.75} \tag{16}$$

where *k* is a constant coefficient.

Determination of k

Due to lack of clinical parameters, the reference of coronary blood flow was derived from simulation in this study. 5 patients with mild stenosis and FFR<0.90 served as references to ensure that the simulation was close to the real physiological value.

Figure 3 shows the technical flow of coronary FFR_{CT}. Firstly, three-dimension model of coronary artery was reconstructed from CCTA. Then, the boundary condition was set as the method mentioned above. Blood was modeled as Newtonian fluid to simulate blood flow in the patient-specific coronary artery tree models, and the blood density and dynamic viscosity were constant at 1050 kg/m^3 and 0.0035 pa • s, respectively [23]. The mesh of the geometries was generated using a non-structural mesh with tetrahedron elements. The standard of 1,000,000 elements was appropriate for simulations by mesh independence test. Simulations were carried out using ANSYS Workbench. Steady flow simulation was employed in this study, which reduced the computational cost significantly. It took within 20 minutes of computational time for one case.

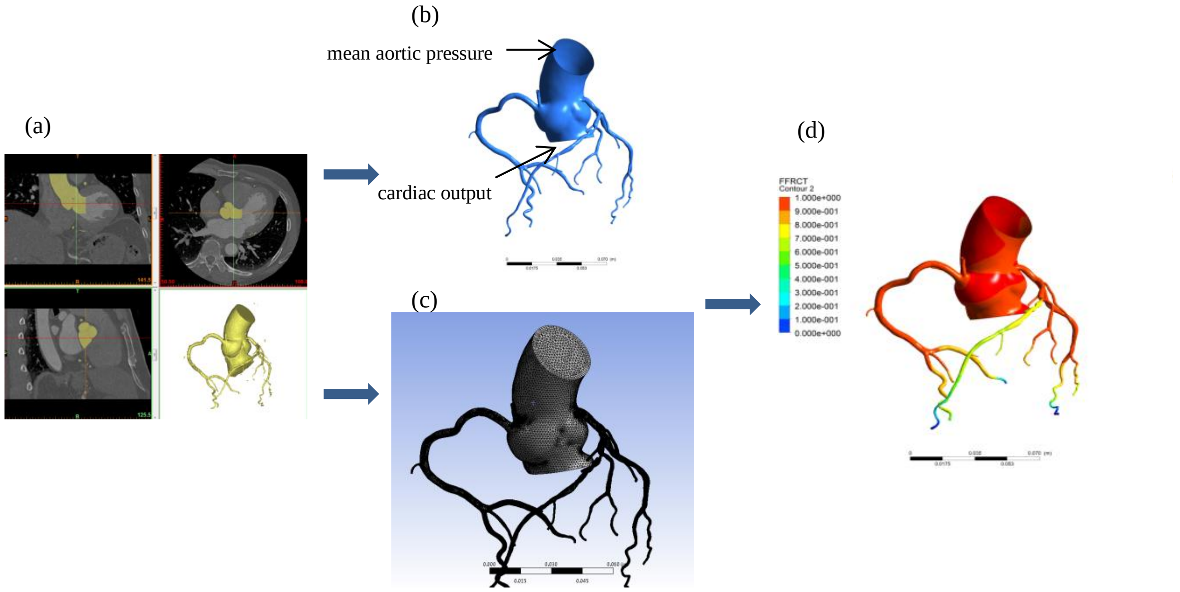

Figure 3. Technical flow chart of coronary FFR_{CT}
(a) 3D reconstruction of coronary artery model based on CCTA; (b) individualized settings of the boundary conditions; (c) meshing of fluid and boundary layer; (d) CFD simulation calculation and post processing

The coronary blood flow was initialized as the product of myocardial mass and myocardial blood flow during hyperemia 3.37 mL/min/g, which is the mean value of human; and then updated as the following steps until the simulation FFR_{CT} matched the invasive FFR.

i. Simulate with the initialization, calculate the coronary FFR_{CT} from the simulation results;

ii. If the simulation FFR_{CT} was larger than invasive FFR, increase the coronary blood flow, otherwise decrease it;

iii. The step-size of adjustment followed by 50, 20, 10, and 5 mL/min, until the simulation FFR_{CT} matched the invasive FFR;

iv. Take the matched one as the reference coronary blood flow.

The reference coronary blood flow was taken into the equation (16) to solve the constant *k*. The mean value of *k* in the 5 patients was taken as the value of *k* in the mathematical model, i.e. *k*=0.003.

Results

Flow division to coronary major branches

Among the 16 patients, 14 cases (88%) were right dominant coronary. The coronary flow division to coronary major branches for the 16 patients was calculated using the vessel volume-based method (Table 1), and they were almost identical to those based on the clinical measurement [24].

Table 1. Comparison of average fraction of coronary flow division over LAD, LCX, and RCA

	LAD (%)	LCX (%)	RCA (%)
Volume-based method	32.9	20.6	46.5
Clinical data	31.1	26.7	41.9

Rationality

Due to lack of clinical coronary blood flow parameters, the ratio of total coronary blood flow in cardiac output (Per_Q) and myocardial blood flow (Q_{myo}) were selected as the evaluation indices to assess the rationality of model of coronary blood flow.

The mean values of Per_Q and Q_{myo} of 16 patients were 16.97% and 4.07 mL/min/g respectively (Table 2 and Table 3), which were in accordance with the rule of medical statistics[25].

Table 2. Summary of Per_Q under model of coronary blood flow

No.	Per_Q (%)	No.	Per_Q (%)
#1	31.85	#9	10.69
#2	17.09	#10	9.67
#3	12.14	#11	14.74
#4	28.79	#12	15.50
#5	10.79	#13	13.35
#6	14.38	#14	14.11
#7	21.58	#15	21.01
#8	21.53	#16	14.22
		Average	*16.97*

Table 3. Summary of Q_{myo} under model of coronary blood flow

No.	Q_{myo} (mL/min/g)	No.	Q_{myo} (mL/min/g)
#1	4.46	#9	3.75
#2	3.94	#10	3.63
#3	4.56	#11	4.61
#4	4.40	#12	4.56
#5	3.68	#13	3.97
#6	2.30	#14	4.79
#7	5.19	#15	3.48
#8	3.94	#16	3.89
		Average	*4.07*

Accuracy

The diagnostic performance of FFR_{CT} was estimated by the reference of clinical coronary FFR, with FFR⩽0.80 as threshold.

Bland-Altman method was used to evaluate the consistency of FFR_{CT} and FFR. The 95% confidence interval between FFR_{CT} and FFR ranges from -0.25 to 0.21, and most of the data fall within the interval, indicating that the two indices have good consistency (Figure 4).

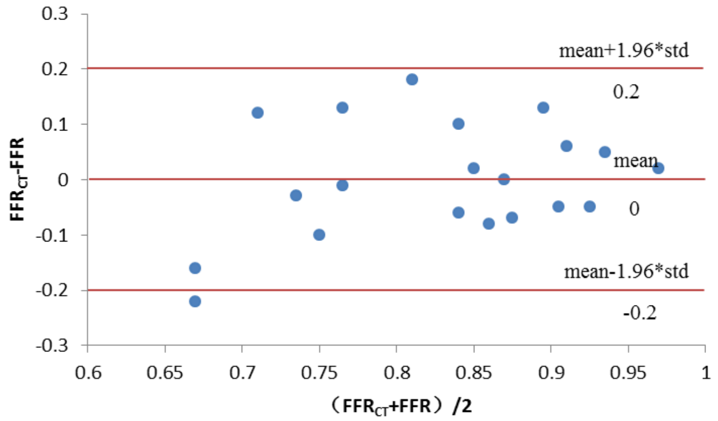

Figure 4. Bland-Altman plot of FFR and FFR_{CT}

Compared with CCTA, which depends only on morphological diagnosis with stenosis rate 50% as ischemic threshold, the diagnostic accuracy of FFR_{CT} was better, i.e. for FFR_{CT} vs CCTA 85% vs 65%, as well as specificity 100% vs. 54.5%, PPV 100% vs. 58.3%, and NPV(78.6% vs. 75% (Table 4).

Table 4. Comparison of the performance between CCTA and FFR_{CT}

Method	Accuracy	Sensibility	Specificity	PPV	NPV
CCTA(50%)	65%	77.8%	54.5%	58.3%	75%
FFR_{CT}(0.80)	85%	66.7%	100%	100%	78.6%

Discussion

This study presented a method of patient-specific flow boundary condition setting orienting to improve the accuracy of coronary FFR_{CT}. The method is simple to operate, and can significantly reduce the time consuming while ensure the accuracy of calculation. A numerical simulation of the calculation takes only 15 minutes with an ordinary PC.

However, there are some limitations in this method. Firstly, the individual difference of coronary microcirculation resistance was not considered. Coronary microcirculation resistance, namely after-loading, which is affected by the activity of the myocardium, affects directly the perfusion of coronary artery. In this study, we supposed that the patients were all with normal coronary microcirculation which had the same response to adenosine and other vasodilator drugs. However, the actual situation is that there is somewhat difference in the coronary microcirculation in different individuals or different regions of individuals, and most of them have different degrees of microcirculatory disturbance [26-27]. Secondly, the model can only be used in the simulation of coronary artery during hyperemia. Whether the model can be applied to rest state still needs to be investigated in-depth. Finally, the simulations in this study are all in steady-state, corresponding to the average condition of hyperemia, so the characteristics of pulsatile blood flow cannot be reflected.

Conclusions

A mathematical method of patient-specific flow boundary condition setting was proposed for the sake of improving the accuracy of coronary FFR_{CT}. By comparing CCTA assessment, coronary FFR_{CT} and invasive FFR, the FFR_{CT} has good consistency with FFR under the patient-specific flow boundary condition. This study offers a new way for improving the accuracy of FFR_{CT}, as well as promoting the clinical application of FFR_{CT}.

Acknowledgement: This work was supported by National Natural Science Foundation of China (11472023, 81301221), and by Program for Liaoning Innovative Research Team in University (LT2014017).

References

[1] Taylor, C. A., Fonte, T. A., & Min, J. K. (2013). Computational fluid dynamics applied to cardiac computed tomography for noninvasive quantification of fractional flow reserve: scientific basis. *Journal of the American College of Cardiology, 61*(22), 2233.

[2] Min, J. K., Taylor, C. A., Achenbach, S., Koo, B. K., Leipsic, J., & Nørgaard, B. L., et al. (2015). Noninvasive fractional flow reserve derived from coronary ct angiography: clinical data and scientific principles. *Jacc Cardiovascular Imaging, 8*(10), 1209-22.

[3] Kleiman, N. S. (2011). Bringing it all together: integration of physiology with anatomy during cardiac catheterization. *Journal of the American College of Cardiology, 58*(12), 1219-1221.

[4] Koo, B. K., Erglis, A., Doh, J. H., Daniels, D. V., Jegere, S., & Kim, H. S., et al. (2011). Diagnosis of ischemia-causing coronary stenoses by noninvasive fractional flow reserve computed from coronary computed tomographic angiograms. results from the prospective multicenter discover-flow (diagnosis of ischemia-causing stenoses obtained via nonin. *Journal of the American College of Cardiology, 58*(19), 1989-97.

[5] Min, J. K., Koo, B. K., Erglis, A., Doh, J. H., Daniels, D. V., & Jegere, S., et al. (2012). Effect of image quality on diagnostic accuracy of noninvasive fractional flow reserve: results from the prospective multicenter international discover-flow study. *Journal of cardiovascular computed tomography, 6*(3), 191.

[6] Min, J. K., Berman, D. S., Budoff, M. J., Jaffer, F. A., Leipsic, J., & Leon, M. B., et al. (2011). Rationale and design of the defacto (determination of fractional flow reserve by anatomic computed tomographic angiography) study. *Journal of Cardiovascular Computed Tomography, 5*(5), 301.

[7] Min, J. K., Leipsic, J., Pencina, M. J., Berman, D. S., Koo, B. K., & Mieghem, C. V., et al. (2012). Diagnostic accuracy of fractional flow reserve from anatomic ct angiography. *Jama the Journal of the American Medical Association, 308*(12), 1237.

[8] Nakazato, R., Park, H. B., Berman, D. S., Gransar, H., Koo, B. K., & Erglis, A., et al. (2013). Noninvasive fractional flow reserve derived from computed tomography angiography for coronary lesions of intermediate stenosis severity results from the defacto study. *Circulation Cardiovascular Imaging, 6*(6):881-889.

[9] Leipsic, J., Yang, T. H., Thompson, A., Koo, B. K., Mancini, G. B., & Taylor, C., et al. (2014). Ct angiography (cta) and diagnostic performance of noninvasive fractional flow reserve: results from the determination of fractional flow reserve by anatomic cta (defacto) study. *American Journal of Roentgenology, 202*(5), 989-94.

[10] Gaur, S., Achenbach, S., Leipsic, J., Mauri, L., Bezerra, H. G., & Jensen, J. M., et al. (2013). Rationale and design of the heartflownxt (heartflow analysis of coronary blood flow using ct angiography: next steps) study. *Journal of Cardiovascular Computed Tomography, 7*(5), 279-288.

[11] Nørgaard, B. L., Leipsic, J., Gaur, S., Seneviratne, S., Ko, B. S., & Ito, H., et al. (2014). The nxt trial (analysis of coronary blood flow using ct angiography: next steps). *Journal of the American College of Cardiology,63*(12), 1145-55.

[12] Miyoshi, T., Osawa, K., Ito, H., Kanazawa, S., Kimura, T., & Shiomi, H., et al. (2015). Non-invasive computed fractional flow reserve from computed tomography (ct) for diagnosing coronary artery disease.*Circulation Journal, 79*(2), 406-12.

[13] Choy, J. S., & Kassab, G. S. (2008). Scaling of myocardial mass to flow and morphometry of coronary arteries. *Journal of Applied Physiology,104*(5), 1281-6.

[14] Arthurs, C. J., Lau, K. D., Asrress, K. N., Redwood, S. R., & Figueroa, C. A. (2016). A mathematical model of coronary blood flow control: simulation of patient-specific three-dimensional hemodynamics during exercise. *American Journal of Physiology - Heart and Circulatory Physiology, 310*(9), H1242-H1258.

[15] Seiler, C., Gould, K. L., & Kirkeeide, R. L. (1992). Basic structure-function relations of the epicardial coronary vascular tree. basis of quantitative coronary arteriography for diffuse coronary artery disease.*Circulation, 85*(6), 1987-2003.

[16] Seiler, C., Kirkeeide, R. L., & Gould, K. L. (1993). Measurement from arteriograms of regional myocardial bed size distal to any point in the coronary vascular tree for assessing anatomic area at risk ☆. *Journal of the American College of Cardiology, 21*(3), 783.
[17] Lee, K. E., Kwon, S. S., Ji, Y. C., Shin, E. S., Choi, J. H., & Kim, S. J., et al. (2016). Estimation of the flow resistances exerted in coronary arteries using a vessel length-based method. *Pflügers Archiv - European Journal of Physiology, 468*(8), 1-10.
[18] Murray, C. D. (1926). The physiological principle of minimum work i. the vascular system and the cost of blood volume. *Proceedings of the National Academy of Sciences, 12*(3), 207.
[19] Abe, M., Tomiyama, H., Yoshida, H., & Doba, N. (2000). Diastolic fractional flow reserve to assess the functional severity of moderate coronary artery stenoses: comparison with fractional flow reserve and coronary flow velocity reserve. *Circulation, 102*(19), 2365-2370.
[20] Yang, M., Shen, X., & Chen, S. (2000). Assessment of the effect of pulmonary hypertension on right ventricular volume and free wall mass by dynamic three-dimensional voxel imaging of echocardiography. *Chinese Journal of Uitrasonography*. *7*:401-404.
[21] Lorenz, C. H., Walker, E. S., Morgan, V. L., Klein, S. S., & Jr, G. T. (1999). Normal human right and left ventricular mass, systolic function, and gender differences by cine magnetic resonance imaging. *Journal of Cardiovascular Magnetic Resonance, 1*(1), 7.
[22] Zhao, Y. X., Liu, J. M., Xu, D. G., Yan, X. B., Lu, L. C., & Xiao, S. Z., et al. (2013). population based study of change trend of the ratio of diastolic to systolic duration during exercise. *Chinese journal of applied physiology, 29*(2), 134.
[23] Zhang, J. M., Zhong, L., Luo, T., Mae, L. A., Huo, Y., & Jonathan, Y., et al. (2016). Simplified models of non-invasive fractional flow reserve based on ct images:. *Plos One, 11*(5), e0153070.
[24] Sakamoto, S., Takahashi, S., Coskun, A. U., Papafaklis, M. I., Takahashi, A., & Saito, S., et al. (2013). Relation of distribution of coronary blood flow volume to coronary artery dominance. *American Journal of Cardiology, 111*(10), 1420-1424.
[25] Uren, N. G., Melin, J. A., De, B. B., Wijns, W., Baudhuin, T., & Camici, P. G. (1994). Relation between myocardial blood flow and the severity of coronary-artery stenosis. *New England Journal of Medicine, 330*(25), 1782-8.
[26] Layland, J. J., Whitbourn, R. J., Burns, A. T., Somaratne, J., Leitl, G., & Macisaac, A. I., et al. (2012). The index of microvascular resistance identifies patients with periprocedural myocardial infarction in elective percutaneous coronary intervention. , *98*(20), 1492-1497.
[27] Erkol, A., Pala, S., Kırma, C., Oduncu, V., Dündar, C., & Izgi, A., et al. (2011). Relation of circulating osteoprotegerin levels on admission to microvascular obstruction after primary percutaneous coronary intervention. *American Journal of Cardiology, 107*(6), 857-62.